Position, momentum, and phasespace oneelectron densities of H2, N2, and LiH

James L. Anchell and John E. Harriman

Citation: The Journal of Chemical Physics **89**, 6860 (1988); doi: 10.1063/1.455360
View online: http://dx.doi.org/10.1063/1.455360
View Table of Contents: http://scitation.aip.org/content/aip/journal/jcp/89/11?ver=pdfcov
Published by the AIP Publishing

Position, momentum, and phase-space one-electron densities of H_2, N_2, and LiH

James L. Anchell and John E. Harriman
Theoretical Chemistry Institute, University of Wisconsin, Madison, Wisconsin 53706

(Received 22 June 1988; accepted 25 August 1988)

Electronic position and momentum densities are commonly used to study bonding. The Husimi function, a phase-space density, complements our understanding of these usual densities. Its value at position **q** and momentum **k** gives the probability for finding an electron in a Gaussian wave packet state centered at **q**, **k**. We have examined these functions for H_2, LiH, and N_2. We find that the Husimi function provides a useful physical decomposition of coordinate density differences into regions labeled by the momentum and of momentum density or density difference into contributions from different spatial regions.

I. INTRODUCTION

The wave function for a quantum system is not observable,[1] although its squared magnitude provides a probability density that is in principle observable. For a many-electron system we must also take into account the fact that only properties depending on one or two electrons at a time are in practice observable. They are determined by the one- and two-electron reduced density matrices. We will limit the present treatment to the one electron case, although most of the formalism could readily be extended to two electrons. In addition, we will not be concerned here with spin effects. We are thus considering the information contained in the one-electron spinless or charge density matrix, which we will refer to simply as the density matrix.

The density matrix is probably best expressed in terms of its natural orbitals, but neither the natural orbitals nor the density matrix elements are observables. In addition, it is difficult to associate a direct physical interpretation with the double set of variables (**r** and **r**′) in the density matrix. We can set **r**′ equal to **r** to obtain the electron (coordinate) density or transform to a momentum representation and then set **p**′ equal to **p** to obtain the momentum density. These densities provide easily visualized information about the electrons in an atom or molecule and they are experimental observables. There is a very long history of the determination of electron densities by x-ray or electron diffraction.[2] More recently, but still with a long history, Compton scattering[3] and $e, 2e$ scattering[4] provide experimental determinations of momentum density distributions.

A knowledge of these two densities does not provide complete information about the density matrix, however. It is of interest to be able to examine the correlation (in the statistical sense[5]) between coordinate and momentum behavior. In addition to knowing total densities, we would like to know the momentum distribution for electrons in a particular spatial region and the distribution in space of electrons with a particular momentum.

In classical mechanics one may define a joint distribution which gives, for an ensemble of systems of particles, the probability density for finding a particle located at a point (**r**,**p**) in phase space. This phase-space density has the properties that it is everywhere positive, and has as its marginal distributions the coordinate- and momentum-space densities. The most common quantum phase-space function, the Wigner function,[6] has the coordinate and momentum densities as marginals[7] but is not itself in general positive and therefore cannot be interpreted as a probability density. Although one can in principle construct an infinite number of positive distributions with the right marginals,[8] such distributions are not linearly related to the density matrix. The uncertainty principle is at the heart of these difficulties, as it disallows the possibility of constructing a quantum distribution which gives the probability of finding a particle located sharply at (**r**,**p**). This difficulty can be avoided if one considers a distribution giving the probability of finding a particle in a Gaussian wave packet state *centered* at the point (**q**,**k**).[9] Such a distribution is the Husimi function given formally by[10–12]

$$\eta(\mathbf{q},\mathbf{k},\sigma) = \frac{1}{(2\pi)^3}\int\int \phi^*(\mathbf{q},\mathbf{k},\sigma|\mathbf{r})\gamma(\mathbf{r};\mathbf{r}') \times \phi(\mathbf{q},\mathbf{k},\sigma|\mathbf{r}')d\mathbf{r}'\,d\mathbf{r}\,, \tag{1}$$

where $\gamma(\mathbf{r};\mathbf{r}')$ is the one-electron charge density matrix and $\phi(\mathbf{q},\mathbf{k},\sigma|\mathbf{r})$ is a Gaussian wave packet in the **r** representation centered at **q** and **k** with width σ:

$$\phi(\mathbf{q},\mathbf{k},\sigma|\mathbf{r}) = \left(\frac{\sigma^2}{\pi}\right)^{3/4}\exp\left[-\frac{\sigma^2}{2}(\mathbf{r}-\mathbf{q})^2 + i\mathbf{k}\cdot\mathbf{r}\right]. \tag{2}$$

Alternatively, the Husimi function may be expressed equally well as

$$\eta(\mathbf{q},\mathbf{k},\sigma) = \frac{1}{2\pi^3}\int\int \tilde{\phi}^*(\mathbf{q},\mathbf{k},\sigma|\mathbf{p})\tilde{\gamma}(\mathbf{p};\mathbf{p}')\tilde{\phi}(\mathbf{q},\mathbf{k},\sigma|\mathbf{p}')d\mathbf{p}'\,d\mathbf{p}\,, \tag{3}$$

where $\tilde{\phi}(\mathbf{q},\mathbf{k},\sigma|\mathbf{p})$ and $\tilde{\gamma}(\mathbf{p},\mathbf{p}')$ are the Gaussian wave packet and the density matrix in the momentum representation.[11] Applications of the Husimi function to atomic systems and elucidation of properties and relationships to other functions (e.g., the Wigner function, the density matrix, the Moyal function) have been investigated in a previous paper.[10] The relationship of the Husimi function to the position and momentum densities is discussed below.

The "observability" of the Wigner function has been discussed by Royer.[13,14] It is surely observable in principle, since the value of the Wigner function at a point in phase space is the expectation value of a Hermitian operator pos-

 0021-9606/88/236860-10$02.10

sessing a complete set of eigenfunctions.[15] The procedure suggested by Royer amounts, however, to observing the Husimi function and then calculating the Wigner function from it.[16] The Husimi function definition in Eq. (1) is equivalent to the expectation value of a projection operator onto the state described by the Gaussian wave packet. While we are not in a position to propose a specific experimental technique and Royer's discussion is in general terms, it seems that this expectation value is much more amenable to experimental evaluation than anything giving the Wigner function directly or an expectation value that might be concocted to give the density matrix. The Gaussian convolutions we will encounter below are in fact likely to be consistent with experimental limitations. We are concerned in this paper with the Husimi function as a way of interpreting theoretical results that is close to physically intuitive ideas and is not tied to a particular theoretical model.

Coordinate and momentum densities of molecular systems have often been explored by decomposing them into orbital contributions. Such contributions cannot be experimentally separated, and the orbitals themselves are defined only within particular calculational models.[17] The Husimi function provides an alternative decomposition of the coordinate space density in terms of its various sections in momentum space and vice versa. This is conceptual useful and is more closely related to experimental observation.

The one-electron phase-space density is defined on a six-dimensional space—three dimensions devoted to the position and three to the momentum coordinates of the electron. By averaging over the angles of the momentum-vector dependence in the Husimi function one obtains a reduced distribution function which depends only on the components of position and the magnitude of the momentum, four variables. From previous work[10] we know that for simple systems the Husimi distribution usually depends weakly on the orientation of the electron momentum and strongly on the magnitude of the momentum. In this paper we explore both the full, six-dimensional and momentum-isotropic Husimi functions.

In this paper we investigate the one-electron phase-space, coordinate-space, and momentum-space distributions of three molecular species: H_2, LiH, and N_2. Total densities, as well as molecular minus superimposed atomic difference densities are explored at different bond lengths. The density matrices for H_2, and N_2 were calculated using GAUSSIAN 82 with a 6-311G (N_2), or 6-311G** (H_2) basis set at the CI singles and doubles level.[18,19] The density matrices for LiH were calculated using GAMESS with a 6-311G basis and single through quadruple excitations.[20] The atomic calculations involved the same basis sets and programs as the molecules in which these atoms occurred. The atomic calculation for Li was at the single-determinant UHF level, whereas the calculation for N was at the CISD level.

II. FORMALISM

A. Position and momentum densities

Although the Husimi function does not possess the position and momentum densities as marginals, its marginals are simply related to these quantities. Consider the marginal $\rho_\sigma(\mathbf{q})$,

$$\rho_\sigma(\mathbf{q}) = \int \eta(\mathbf{q},\mathbf{k},\sigma)\, d\mathbf{k}\,. \tag{4}$$

Substitution of the Husimi function defined by Eq. (1) gives

$$\rho_\sigma(\mathbf{q}) = \frac{1}{(2\pi)^3}\left(\frac{\sigma^2}{\pi}\right)^{3/2}\int\int \gamma(\mathbf{r},\mathbf{r}') \times\exp\left[-\frac{\sigma^2}{2}(\mathbf{r}-\mathbf{q})^2 - \frac{\sigma^2}{2}(\mathbf{r}'-\mathbf{q})^2\right] \times\int \exp i\mathbf{k}\cdot(\mathbf{r}-\mathbf{r}')\, d\mathbf{k}\, d\mathbf{r}\, d\mathbf{r}'\,. \tag{5}$$

The integration over $\mathbf{k}$ gives $(2\pi)^3\delta(\mathbf{r}-\mathbf{r}')$, so that Eq. (5) becomes

$$\rho_\sigma(\mathbf{q}) = \int \rho(\mathbf{r})\Phi(\sigma|\mathbf{r}-\mathbf{q})d\mathbf{r}\,,$$
$$\Phi(\sigma|\mathbf{r}-\mathbf{q}) = \left(\frac{\sigma^2}{\pi}\right)^{3/2}\exp[-\sigma^2(\mathbf{r}-\mathbf{q})^2]\,, \tag{6}$$

where we have identified $\gamma(\mathbf{r};\mathbf{r})$ with the one-electron coordinate density $\rho(\mathbf{r})$, and Φ is a normalized Gaussian distribution. Equation (6) reveals that the marginal of the Husimi function with respect to integration over $\mathbf{k}$ is a Gaussian convolution of the one-electron coordinate density. Alternatively, if one begins with the definition of the Husimi function as expressed in Eq. (3), it is possible to show that the marginal of the Husimi function related to integration over $\mathbf{q}$ is a Gaussian convolution of the momentum density, $\pi(\mathbf{p})$:

$$\pi_\sigma(\mathbf{k}) = \int \pi(\mathbf{p})\Phi(\sigma^{-1}|\mathbf{p}-\mathbf{k})d\mathbf{p}\,. \tag{7}$$

Another connection exists between the Husimi function and the coordinate- and momentum-space densities that provides insight to the role of σ. Consider the function $\pi(\mathbf{k})$ defined by

$$\pi(\mathbf{k}) = \lim_{\sigma\to 0}\left(\frac{\pi}{\sigma^2}\right)^{3/2}\eta(\mathbf{q},\mathbf{k},\sigma)\,. \tag{8}$$

Using the definition given by Eq. (1) in Eq. (8) we find

$$\pi(\mathbf{k}) = (2\pi)^{-3}\lim_{\sigma\to 0}\int\int \gamma(\mathbf{r};\mathbf{r}')\exp\left[-\frac{\sigma^2}{2}(\mathbf{r}-\mathbf{q})^2 - \frac{\sigma^2}{2}(\mathbf{r}'-\mathbf{q})^2\right]\exp i\mathbf{k}\cdot(\mathbf{r}'-\mathbf{r})d\mathbf{r}'\, d\mathbf{r}\,, \tag{9}$$

which implies that

$$\pi(\mathbf{k}) = (2\pi)^{-3}\int\int \gamma(\mathbf{r};\mathbf{r}')\exp[i\mathbf{k}\cdot(\mathbf{r}'-\mathbf{r})]d\mathbf{r}'\, d\mathbf{r}\,. \tag{10}$$

The double integration in Eq. (10) Fourier transforms the variables $\mathbf{r}$ and $\mathbf{r}'$ to $\mathbf{k}$, so that

$$\pi(\mathbf{k}) = \tilde{\gamma}(\mathbf{k};\mathbf{k})\,, \tag{11}$$

which is the one electron momentum density. Similarly, starting with the definition of the Husimi function given by Eq. (3) one can show that the one-electron coordinate density can be expressed as

$$\rho(\mathbf{q}) = \lim_{\sigma\to\infty}(\pi\sigma^2)^{3/2}\eta(\mathbf{q},\mathbf{k},\sigma)\,. \tag{12}$$

This discussion clarifies the role of the wave packet width parameter σ in the Husimi function: as σ tends toward zero the phase-space distribution becomes sharper in coordinate space, and as σ tends towards infinity the distribution becomes sharper in momentum space. This phenomena is readily understood if one recalls the expressions for the uncertainty in $\mathbf{q}$ and $\mathbf{p}$ for a Gaussian wave packet with width σ, i.e.,

$$\Delta q_\alpha = \frac{1}{\sqrt{2\sigma_\alpha}}, \quad \Delta p_\alpha = \frac{\sigma_\alpha}{\sqrt{2}}, \tag{13}$$

where α labels one of the three Cartesian directions, x, y, or z. We require that $\sigma_x = \sigma_y = \sigma_z = \sigma$. In order to obtain a quantum phase space distribution which gives equal uncertainty in the position and momentum coordinates one sets σ equal to unity in atomic units (a_0^{-1}). All the Husimi functions presented here have been evaluated with $\sigma = 1$, so we will suppress σ as an argument of the Husimi function.

B. Integration over angles of k

As noted by Thakkar *et al.*[21] the momentum density is essentially a single-center distribution, so a partial wave expansion is appropriate and should converge with reasonable rapidity. We can make a similar expansion of the $\mathbf{k}$ dependence of $\eta(\mathbf{q},\mathbf{k})$:

$$\eta(\mathbf{q},\mathbf{k}) = \sum_{l=0}^{\infty} \sum_{m=-l}^{l} \eta_{lm}(\mathbf{q},k) Y_l^m(\theta_k,\phi_k), \tag{14}$$

where θ_k and ϕ_k denote the angular components of the vector $\mathbf{k}$ in a coordinate system in which the q_z axis is collinear with the internuclear axis. By symmetry, the Husimi function for a diatomic in a Σ state can depend on the variables θ_q and θ_k only through their difference, $\phi_q - \phi_k$. Because of this symmetry ϕ_k may be treated as a constant equal to zero. This consideration leads to values of η_{lm} which are vanishing for $m \neq 0$. If the Husimi function has inversion symmetry with respect to $\mathbf{k}$ then η_{lm} vanishes for all odd l. In the present case it is straightforward to show that $\eta(\mathbf{q},\mathbf{k})$ has this symmetry: First note from Eq. (2) that $\phi(\mathbf{q},-\mathbf{k}) = \phi^*(\mathbf{q},\mathbf{k})$. Also, in general $\gamma^*(\mathbf{r};\mathbf{r}') = \gamma(\mathbf{r}';\mathbf{r})$. However, since the density matrices we are working with are real, interchanging $\mathbf{r}$ and $\mathbf{r}'$ leaves the density matrix unchanged. From Eq. (1), if we let $\mathbf{k}$ go into $-\mathbf{k}$, and subsequently interchange $\mathbf{r}$ and $\mathbf{r}'$, we see from the properties of the wave packet and density matrix described above that the Husimi function remains unchanged. In summary, for the problem at hand, the Husimi function may be expressed as

$$\eta(\mathbf{q},\mathbf{k}) = \sum_{l=0}^{\infty} \eta_{2l}(\mathbf{q},k) P_{2l}(\theta_k). \tag{15}$$

In order to reduce the dimensionality of the space on which the Husimi function is defined, we average over momentum orientation by integrating over the angles of $\mathbf{k}$ and dividing by 4π. From Eq. (15) this leads to

$$\bar{\eta}(\mathbf{q},k) = \frac{1}{4\pi} \int \eta(\mathbf{q},\mathbf{k}) d\hat{\mathbf{k}} = \frac{1}{(4\pi)^{1/2}} \eta_0(\mathbf{q},k). \tag{16}$$

That is, the result of integrating over the angles of $\mathbf{k}$ is proportional to the leading term in the expansion of Eq. (15). To determine how much information is lost in averaging one needs to compare the size of η_0 to the higher order η_{2l}. This was carried out for the atomic case through $2l = 6$ in a previous paper,[10] where it was found that the anisotropic effects were orders of magnitude smaller than the isotropic contribution. The higher-order contributions for diatomic molecules involve equations of considerable length and have yet to be tested. However, by evaluating $\eta(\mathbf{q},\mathbf{k})$ at varying $\mathbf{k}$-vector orientations we have been able to assess which regions of phase space are most nearly isotropic with respect to the orientation of $\mathbf{k}$, and hence which regions of phase space are most amenable to angle averaging.

III. GENERAL FEATURES OF DENSITY PLOTS

For purposes of discussion it is convenient to assign labels to gross regions of coordinate and momentum space. In discussing coordinate space we will refer to three regions: The region between the nuclei and near to the bond axis; the region immediately around the nuclei; and the region near the axis but on the side of either nucleus opposite the other nucleus. These will be referred to as the internuclear, core, and external regions, respectively. In momentum space we refer to momentum directed along the bond axis and perpendicular to the bond axis as longitudinal, and transverse, respectively.

There are several types of contour plots which we have used to study bonding in diatomics. Before analyzing each one on a case-by-case basis, we cite a few features which are common throughout, so as to avoid repetitions later.

A. Total position and momentum densities

Figure 1 shows density difference plots at R_{eq} for N_2, H_2, and LiH. For the nonpolar diatomics, H_2 and N_2, $\Delta\rho(\mathbf{r})$

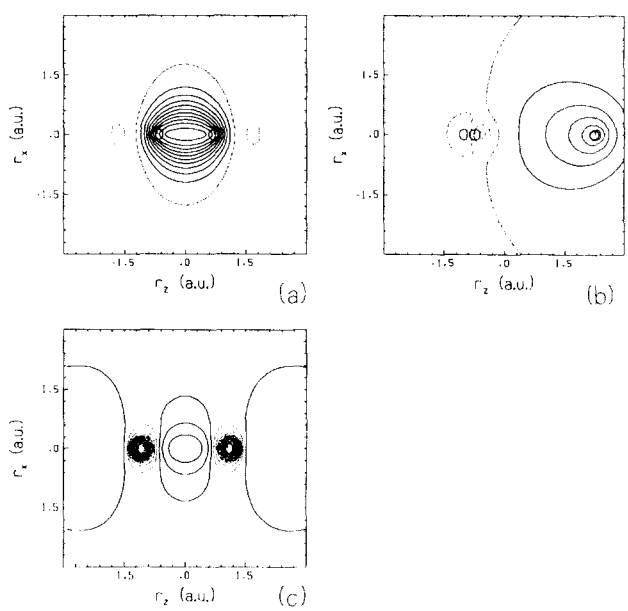

FIG. 1. Coordinate density difference $\Delta\rho(\mathbf{r})$ at R_{eq} for (a) H_2, (b) LiH, and (c) N_2. Contours: (a) -0.01 to 0.1 in steps of 0.01, (b) -0.02 to 0.05 in steps of 0.01, (c) -1.3 to 0.2 in steps of 0.1.

has positive contours (built up density) in the internuclear region. There are negative contours (depleted density) in the external (H_2) or core (N_2) regions. This density transfer is well known.[22] For polar LiH a depletion of charge occurs around the Li nucleus which is compensated for by a buildup of charge around the H nucleus. This transfer of charge is indicative of ionic bonding.

The system energy and the second moment of the momentum density are related by the virial theorem for diatomics[23]:

$$\langle T \rangle = -E - R\frac{dE}{dR}, \tag{17}$$

where $\langle T \rangle$ is the expectation value of the kinetic energy, E is the total energy, and R is the bond length. As the bond is stretched from its equilibrium value the energy becomes less negative, so the first term on the right-hand side of Eq. (17) will contribute to a lowering of $\langle T \rangle$, and consequently of $\langle p^2 \rangle$. Along the soft part of the potential R and dE/dR are always greater than or equal to zero, so the second term also serves to lower $\langle T \rangle$. This is manifested by a contraction of $\pi(\mathbf{p})$ in both the longitudinal and transverse directions.

Another common feature of the momentum-space distributions of diatomics is the bond directionality principle (BDP), which asserts that $\pi(\mathbf{p})$ should be contracted along the longitudinal direction and expanded along the transverse direction. Coulson,[24] who first recognized the BDP, gave a mathematical treatment of the subject.[25] For a singly bonded diatomic he began with a bonding molecular orbital of the form

$$\psi(\mathbf{r}) = \frac{\psi_a(\mathbf{r}) + \psi_b(\mathbf{r})}{[2(1+S)]^{1/2}}, \tag{18}$$

where $\psi_i(\mathbf{r})$ represents an atomic orbital centered on atom i, and S is the overlap of $\psi_a(\mathbf{r})$ and $\psi_b(\mathbf{r})$. From this form Coulson showed that

$$\chi(\mathbf{p})\chi^*(\mathbf{p}) = \frac{1+\cos(\mathbf{p}\cdot\mathbf{R})}{1+S}\chi_{\text{atom}}(\mathbf{P})\chi^*_{\text{atom}}(\mathbf{p}), \tag{19}$$

where $\chi(\mathbf{p})$ and $\chi_{\text{atom}}(\mathbf{p})$ are the momentum representations of ψ and ψ_a, respectively, and $\mathbf{R}$ is the internuclear vector. Since anisotropy will not arise from the spherically symmetric atomic density one sees that the origin of the BDP in the factor multiplying $\chi_{\text{atom}}(\mathbf{p})\chi^*_{\text{atom}}(\mathbf{p})$. This term, called the diffraction factor, not only accounts for the BDP, but also predicts oscillation in the momentum density along the z-axial direction with period $2\pi/R$.[26] This latter effect has been observed in the present work and elsewhere—both theoretically and experimentally.[27,28] A simple physical explanation of the BDP goes as follows.[29] Because of the charge transfer described earlier for nonpolar diatomics, the charge density and the total wave function for the system are slowly changing along the bond axis. Conversely, perpendicular to the axis the wave function should fall off quickly. Recalling that the momentum-space wave function is the Fourier transform of the position-space wave function, and that the Fourier transform of a function converts diffuse regions into sharp regions and vice versa, one sees the origin of the BDP.

The BDP is clearly illustrated in Fig. 2 for the homonuclear diatomics, although the situation is more complicated for N_2, because of other contributions to be discussed later in Sec. VI. The polar molecule LiH does not show the BDP, as the arguments given in the previous paragraph do not apply. (See Sec. V.)

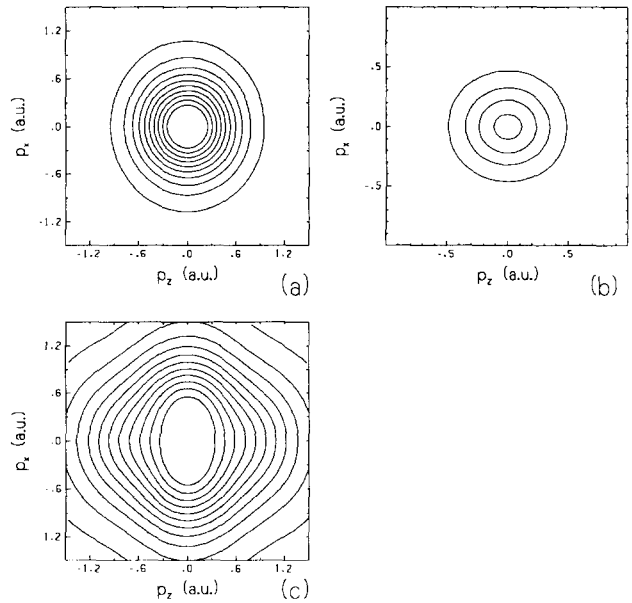

FIG. 2. Total momentum densities $\pi(\mathbf{p})$ at R_{eq} for (a) H_2, (b) LiH, and (c) N_2. Contours: (a) 0.1 to 1.1 in steps of 0.1, (b) 1 to 4 in steps of 1, (c) 0.1 to 1.1 in steps of 0.1.

B. Phase space density

The Husimi function is a joint coordinate- and momentum-space distribution. One of the easiest ways to begin to understand the Husimi function is to observe a coordinate space density for which the momentum of the electron has been specified. For example, Fig. 3 shows the angle-averaged Husimi function, $\bar{\eta}(\mathbf{q},k)$ for LiH at R_{eq}. Sections with $k=0$ and $k=4.5$ are included.[30] Not surprisingly, the most probable place to find fast electrons is near the Li nucleus, where the external (or nuclear) potential is most negative.

Husimi function difference densities $\Delta\eta(\mathbf{q},\mathbf{k})$ or $\Delta\bar{\eta}(\mathbf{q},k)$ may also be considered. [Most of the general properties of $\Delta\eta(\mathbf{q},\mathbf{k})$ hold as well for $\Delta\bar{\eta}(\mathbf{q},\mathbf{k})$, so for the remainder of this paper, we will use $\Delta\eta$ to represent either $\Delta\eta(\mathbf{q},\mathbf{k})$

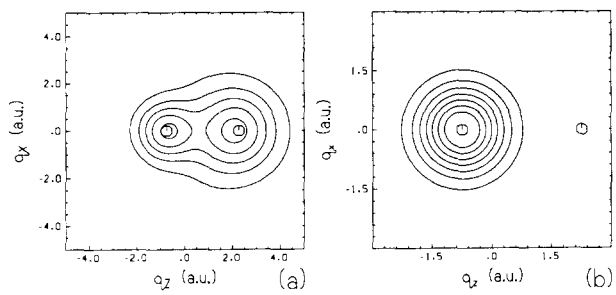

FIG. 3. Angle-averaged Husimi function for LiH at R_{eq} (a) $k=0$ and (b) $k=4.5$. Contours: (a) 1×10^{-5} to 5×10^{-5} in steps of 10^{-5}, (b) 1×10^{-5} to 7×10^{-5} in steps of 10^{-5}.

or $\Delta\bar{\eta}(\mathbf{q},k)$ unless otherwise specified.] There is a tendency for $\Delta\eta(\mathbf{q},\mathbf{k})$ for fixed $\mathbf{k}$ of small magnitude to qualitatively resemble $\Delta\rho(\mathbf{r})$, but there are exceptions. The ability to look at coordinate densities as a function of k allows us to see effects that are washed out in the total density plots.

An important distinction should be made between $\Delta\eta$ sections and $\Delta\rho(\mathbf{r})$. In a total density difference plot one may assert that the regions of depletion are exactly compensated for by the regions of buildup—that the integral of $\Delta\rho(\mathbf{r})$ or $\Delta\pi(\mathbf{p})$ over all r space or p space should be zero. For $\Delta\eta$ densities that are sections for fixed $\mathbf{k}$ or k, one cannot make this claim. The depletion of density occurring at one value of k may appear as a buildup, or partial buildup, of density at the same k value or another k value—it is the integral over both k and q space which makes $\Delta\eta$ vanish.

However, using the momentum density difference $\Delta\pi(\mathbf{p})$ one can get a sense of the overall displacement of the electron momentum. This function is shown in Fig. 4 for LiH and for N_2. The overall shift from low to high momentum is apparent and a similar shift is observed in H_2 at R_{eq}. The $\Delta\pi$ contours do not indicate *where* the electrons were that underwent a change in momentum, only that in the formation of a bond it is probable that the electron momentum increased. If a net depletion is observed in a $\Delta\eta$ cross section for a given k, it is reasonable to assume that this will be compensated for by a net buildup in $\Delta\eta$ with larger k. This is observed for LiH: For all k greater than about six the $\Delta\eta$ plots show only positive contour regions. These positive regions must be compensated for by depletions of density *somewhere*, and the only depletions occur at lower k.

For other systems $\Delta\pi(\mathbf{p})$ may indicate that the total momentum is being shifted in the opposite direction, or that a particular component of the momentum is being preferentially shifted.

IV. H_2

A. Position and momentum densities

The momentum density of H_2 at $R = 7$ in Fig. 5 shows three local maxima, at p_z equal to 0 and approximately ± 0.7. From Eq. (19) one observes that as R increases the period of oscillation in $\pi(\mathbf{p})$ decreases. Consequently, for small R one may not observe oscillations in $\pi(\mathbf{p})$ because (a) the period of oscillation may be greater than the range of p_z chosen for study; and (b) even if $\pi(\mathbf{p})$ were evaluated at large R the oscillations would be damped so greatly as not to be visible without considerable magnification.

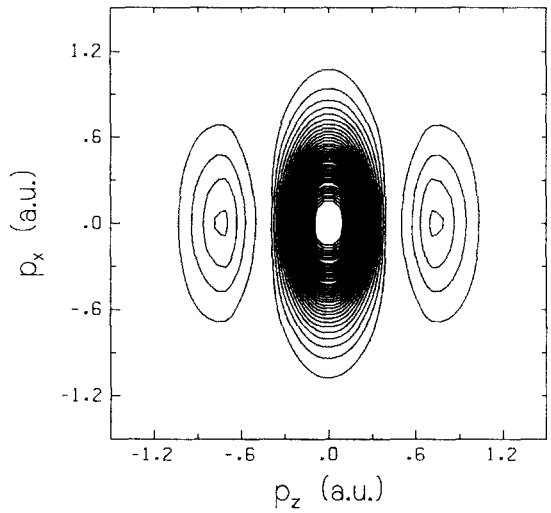

FIG. 5. Total momentum density $\pi(\mathbf{p})$ for H_2 at $R = 7$. Contours: 0.1 to 2.8 in steps of 0.1.

The momentum density difference $\Delta\pi(\mathbf{p})$, shown in Fig. 6, undergoes a radical change as R is varied. At $R_{eq} = 1.405$ an overall shift from low momentum to high momentum occurs. At $R = 5$ the momentum density shifts from high momentum to low momentum. Further, at R_{eq} the shift in momentum occurs primarily in the transverse direction, whereas at $R = 5$ the shift is in the longitudinal direction. These shifts can be understood by considering $\Delta\rho(\mathbf{r})$ at R_{eq} (Fig. 1) and $R = 5$ (Fig. 7). At R_{eq}, $\Delta\rho(\mathbf{r})$ shows that electron density is transferred from an external (low momentum) region to internuclear and core (higher momentum) regions. At $R = 5$ we witness the transfer of electron density from around the core (high momentum) region to the center of the internuclear region, which is now a low momentum region due to its relative distance from the nuclei. The anisotropic depletion of momentum density observed at $R = 5$ is consistent with other studies. In particular, Ruedenberg[31] showed for H_2^+ that (a) as R is decreased $\langle T \rangle$ initially decreases and then increases, and it is this initial decrease which creates stability in the molecule at large R; and (b) a decomposition of $\langle T \rangle$ into longitudinal and transverse components—$T_\parallel$ and $T_\perp$, respectively—reveals that $T_\perp$ remains fairly constant, and that it is $T_\parallel$ which mostly contributes to the overall lowering of $\langle T \rangle$.

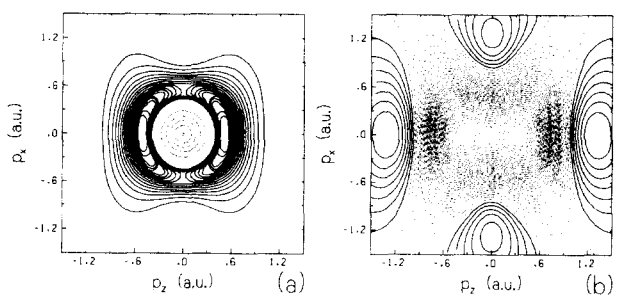

FIG. 4. Momentum density difference $\Delta\pi(\mathbf{p})$ at R_{eq} for (a) LiH and (b) N_2. Contours: (a) -5 to -1 in steps of 1 and 0.01 to 0.18 in steps of 0.01, (b) -0.32 to 0.07 in steps of 0.01.

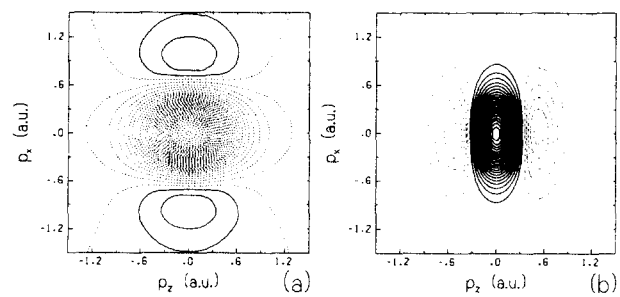

FIG. 6. Momentum density difference $\Delta\pi(\mathbf{p})$ for H_2 at (a) R_{eq} and (b) $R = 5$. Contours: (a) -0.3 to 0.02 in steps of 0.01, (b) -0.5 to 2.2 in steps of 0.1 (zero excluded).

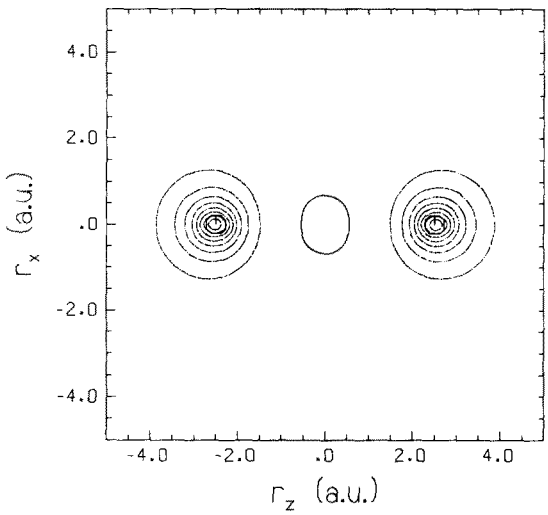

FIG. 7. Coordinate density difference $\Delta\rho(\mathbf{r})$ for H_2 at $R = 5$. Contours: -0.075 to 0.005 in steps of 0.01.

B. Husimi distribution

1. Isotropic Husimi function

The angle-averaged Husimi difference function for H_2 at R_{eq} is shown in Fig. 8. We observe in $\Delta\bar{\eta}(\mathbf{q},\mathbf{k})$ for $k \lesssim 1.9$ the same type of redistribution observed in $\Delta\rho(\mathbf{r})$. That is, we see a depletion of density in the external region and a buildup of density in the internuclear region. We shall refer to this common type of contour as a *forward redistribution*. As the bond length is varied the range over which forward redistribution occurs varies considerably. For example, at $R = 1$ we observe forward redistribution up to approximately $k = 2.9$, but for $R = 2$ forward redistribution occurs only up to about $k = 1.4$. Certainly, one of the biggest changes occurring in H_2 as the bond length is increased is that the external potential in the internuclear region becomes less negative. As this potential is increased we expect the expectation value of the kinetic energy of the electron to decrease. There seems then to be an obvious correlation between the magnitude of $\langle T \rangle$ and the magnitude of the range over which forward redistribution occurs in the phase space defined by the Husimi function. From another viewpoint we could say that the range of k in $\Delta\bar{\eta}(\mathbf{q},k)$ which most closely mimics $\Delta\rho(\mathbf{r})$ is decreased as the bond is stretched.

For larger values of k we find a stronger dependence of $\eta(\mathbf{q},\mathbf{k})$ on the orientation of $\mathbf{k}$, so we turn to the anisotropic Husimi function for further analysis of the phase space.

2. Anisotropic Husimi function

For certain ranges of very large k the Husimi difference contour plots show a reversal in the density redistribution. For example, for k in the range of 3.1 to 4.4 a depletion of electron density in the internuclear region and a buildup of density in the external region occurs in H_2 at R_{eq}. We will refer to this type of redistribution as a *reverse redistribution*. The reverse redistribution can be observed with the angle-averaged Husimi function, but the electron densities in the regions of phase space where reverse redistributions occur are highly anisotropic, so we make use of the full six-dimensional Husimi function to study this behavior. If we choose $\mathbf{k}$ perpendicular to the bond, so that $k_x = 4$, $k_y = 0$, and $k_z = 0$ [or more succinctly, $\mathbf{k} = (4,0,0)$], then the resulting density difference section shows only global buildup of charge density. Choosing $\mathbf{k}$ parallel to the bond [i.e., $\mathbf{k} = (0,0,4)$] results in a density difference plot with a reverse redistribution (see Fig. 9). Further understanding of this phenomenon may be gained from a study of the cross section of the six-dimensional Husimi function obtained by setting all variables except q_z and k_z equal to zero (Fig. 10). At R_{eq} and k_z less than 3 a.u. only forward redistribution occurs along the z axis. But for k_z in the range of 3.1 to 4.4 the H_2 molecule is in a region of reverse redistribution. For values of k_z greater than 4.4 only global regions of buildup occur along the z axis. If we compress the bond to one atomic unit we see that the region of reverse redistribution has expanded to include values of k_z between 3.0 and 5.2. Further, the positive regions are an order of magnitude larger than they were at R_{eq}. At $R = 2$ the trends go the other way. That is, the range over which reverse redistributions occur is now limited to k_z between 3.5 and 3.8, and the exterior regions of positive buildup are an order of magnitude smaller than they were at R_{eq}. For k_z between 3.8 and 4.8 forward redistribution occurs again, but there continues to be a buildup of charge density in the external region. For k_z greater than 4.8

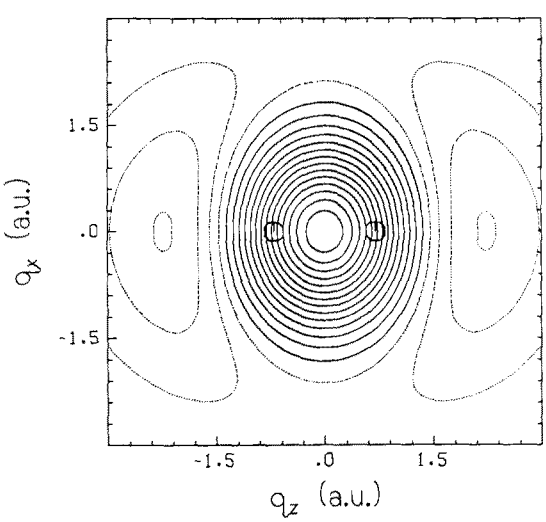

FIG. 8. Angle averaged Husimi function difference $\Delta\bar{\eta}(\mathbf{q},0)$ for H_2 at R_{eq} and $k = 0$. Contours: -3×10^{-4} to 14×10^{-4} by 10^{-4}.

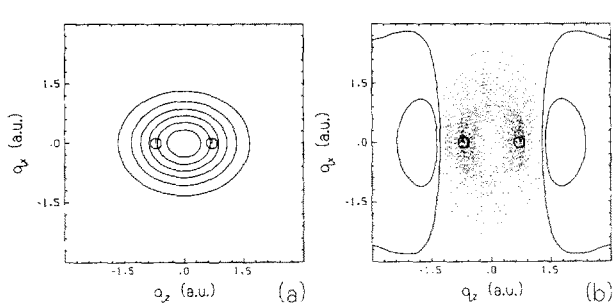

FIG. 9. Fixed-$\mathbf{k}$ sections of the Husimi function difference $\Delta\eta(\mathbf{q},\mathbf{k})$ for H_2 at R_{eq}: (a) $\mathbf{k} = (4,0,0)$ and (b) $\mathbf{k} = (0,0,4)$. Contours: (a) 1×10^{-6} to 6×10^{-6} in steps of 10^{-6}, (b) -28×10^{-7} to 2×10^{-7} in steps of 10^{-7} (zero excluded).

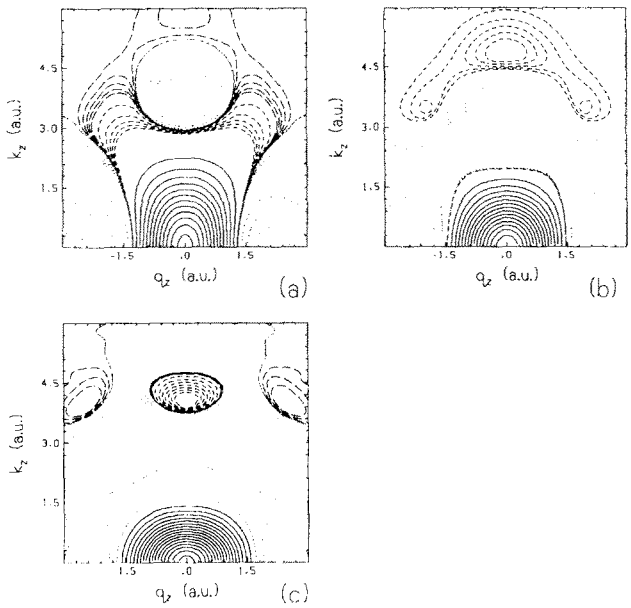

FIG. 10. Husimi function q_z, k_z sections with $q_x = q_y = 0$ and $k_x = k_y = 0$ for H_2 at (a) $R = 1$, (b) R_{eq}, and (c) $R = 2$. Contours: (a) dotted lines and solid lines: -3×10^{-4} to 12×10^{-4} in steps of 10^{-4}; widely spaced dotted lines and dashed lines: -7×10^{-6} to 5×10^{-6} in steps of 10^{-6}; large dashed lines: 1×10^{-7} to 5×10^{-7} in steps of 10^{-7}, (b) dotted lines and solid lines: -3×10^{-4} to 14×10^{-4} in steps of 10^{-4}; widely spaced dotted lines: -1×10^{-6} to 5×10^{-6} in steps of 10^{-6}; dashed lines: 1×10^{7} to 5×10^{-7} in steps of 10^{-7}, (c) dotted lines and solid lines: -2×10^{-4} to 16×10^{-4} in steps of 10^{-4}; widely spaced dotted lines and dashed lines: -3×10^{-7} to 8×10^{7} in steps of 10^{-7}; large dashed lines: 1×10^{-8} to 3×10^{-8} in steps of 10^{-8}.

reverse redistribution recurs. There is then an oscillatory nature to these difference contour distributions. The oscillations occurring at higher k values are small in magnitude, so they may escape notice without magnification. It may be that the reverse redistribution is a response of the core electrons to the increased density in the internuclear region. This shift in the density would create a polarization in the core. In general, we find that as the bond is shortened the electron density redistributes so as to deplete electrons with high momentum moving parallel to the axis from the internuclear region, and to create a buildup of density in the external region. The range of k_z for which this reverse redistribution occurs, and the intensity of redistribution with respect to buildup of electron density is increased as the bond length is shortened.

Sections of $\Delta\eta(\mathbf{q},\mathbf{k})$ with all variables except q_z and k_z set to zero revealed only regions of forward distribution followed by regions of global density increase. This was the case at all values of R studied.

V. LiH

A. Position and momentum densities

Our studies show that at $R_{eq} = 3.029$ (Fig.2) and at $R = 4$ the momentum density of LiH is nearly isotropic—the BDP does not hold. This is not surprising, in view of the ionic nature of LiH. The isotropic nature of the charge density due to two spherical ions is preserved in momentum space by the Fourier transform of the wave function. Of course the ground state of LiH dissociates into neutral Li and H atoms, and by $R = 6$ we find that the momentum density is weakly though noticeably anisotropic, qualitatively similar to that for H_2 (Fig. 2).

Contours of $\Delta\rho(\mathbf{r})$ indicate that at R_{eq} electron density is transferred from the internuclear region near Li to a region around H and to a region external to Li. (See Fig. 1.) At $R = 6$ the charge transfer is from a region centered around Li, and from a region external to Li centered roughly at $r_z = -3$ to the internuclear region, and to a region external to Li centered roughly at $r_z = -2$. The buildup observed in the internuclear region is consistent with our knowledge of the proper dissociation of LiH and with the anisotropic behavior of $\pi(\mathbf{p})$ at $R = 6$.

B. Husimi function

1. Isotropic Husimi function

Figure 11 shows $\Delta\bar{\eta}(\mathbf{q},\mathbf{k})$ at R_{eq} for LiH. At $k = 0$ a region of electron density depletion is observed external to Li, centered around $q_z = -3$. As k is increased the center of this region of depletion moves to more positive values of q_z. (The z axis is directed from Li to H.) At $k = 6$, for example, we find this region of depletion has moved into the internuclear region centered near $q_z = 0$. Correspondingly, electron density buildup appears around H at all values of k studied. We recall that at R_{eq}, $\Delta\rho(\mathbf{r})$ showed a net increase of electron density external to Li (Fig. 1). We see the occurrence of this external buildup in $\bar{\eta}(\mathbf{q},k)$ at large values of k. Around $k \gtrsim 6$ an increase in electron density is observed in this region. From these findings we believe the following occurs in bond formation between Li and H: First, electron density of a wide range of momentum is transferred from Li to H. Second, because of the net negative charge acquired by H, fast (core) electrons near the Li nucleus migrate to the external region away from H. That is, a dipole is induced on Li.

2. Anisotropic Husimi function

Figure 12 shows phase-space sections for LiH at R_{eq}. Figure 12(a) is a q_z *vs* k_z section, and Fig. 12(b) is a q_z vs k_x section. In both cases all remaining phase-space variables are set to zero. In both pictures we see that for $k \lesssim 2.1$ there is a decrease in density around the Li atom and an increase in density near the H atom, this being much the same as the density difference observed in $\Delta\rho(\mathbf{r})$. Beginning around $k = 2.1$ we observe in Fig. 12(a) a decrease in density in the

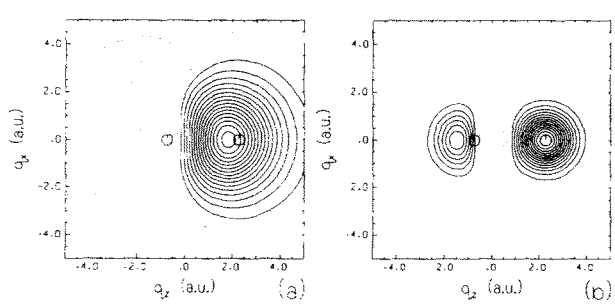

FIG. 11. Angle-averaged Husimi function difference $\Delta\bar{\eta}(\mathbf{q},\mathbf{k})$ for LiH at R_{eq}: (a) $k = 0$ and (b) $k = 6$. Contours: (a) -3×10^{-4} to 16×10^{-4} in steps of 10^{-4}, (b) -4×10^{-9} to 14×10^{-9} in steps of 10^{-9}

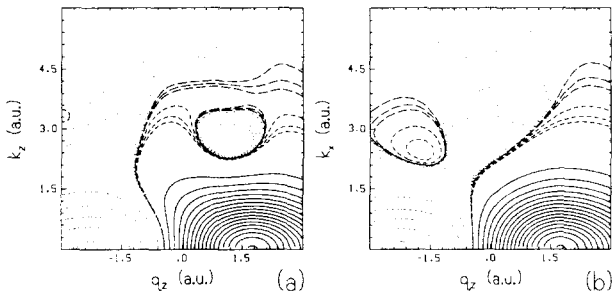

FIG. 12. Husimi function sections for LiH at R_{eq}: (a) q_z, k_z section with $q_x = q_y = 0$, $k_x = k_y = 0$ and (b) q_z, k_x section with $q_x = q_y = 0$, $k_y = k_z = 0$. Contours: (a) dotted lines and solid lines: -5×10^{-4} to 17×10^{-4} in steps of 10^{-4}: widely spaced dotted lines and dashed lines: -3×10^{-6} to 3×10^{-6} in steps of 10^{-6}; most widely spaced dotted lines and large dashed lines: -3×10^{-7} to 3×10^{-7} in steps of 10^{-7}, (b) same as (a).

internuclear region and an increase in density around H and external to the Li atom. This type of redistribution continues through all values of k shown in the section. As k is increased the width of the depleted region expands with respect to its q_z dimension. The buildup of these high momentum electrons that we observe in the external region corresponds to the buildup observed in $\Delta\rho(\mathbf{r})$ seen in this same region of coordinate space.

A different type of redistribution occurs in the q_z *vs* k_x sections. Here the contours do not change qualitatively much until around $k_x = 2.3$. In the range of $k_x = 2.3$ to $k_x = 3.5$ we see that the internuclear region has been divided into a depleted zone near H and a zone of increased density near Li. Above $k_x = 3.5$ the redistribution continues as in the low momentum case (i.e., $k_x \lesssim 2.3$) with the region of depletion growing in width as k_x is increased.

Above $k = 2.1$ we have seen that the phase-space density varies greatly with respect to the orientation of $\mathbf{k}$. Hence for $k > 2.1$ the isotropic Husimi function represents an averaging of quite different distributions. In particular, we noted in the previous section that the occurrence of density depletion in the internuclear region and the buildup of density in the region external to Li did not occur simultaneously until we reached the neighborhood of $k = 6$. Whereas we have just seen that if we focus only on transverse $\mathbf{k}$ that this type of redistribution occurs at lower momentum. One might view this as a weakness in $\Delta\bar{\eta}(\mathbf{q},k)$ because of the information lost in averaging. However, what we have learned from $\Delta\bar{\eta}(\mathbf{q},k)$ in this instance is that the depletion of longitudinally directed electron density in the region external to Li, and the buildup of transversely directed electron density in the same region roughly cancel each other out until higher values of the momentum are reached.

VI. N_2

A. Position and momentum densities

The density difference contour plot for N_2 at $R_{eq} = 2.074$ (Fig. 1) shows reduced density around the cores and increased density in the internuclear and external regions. The momentum density at R_{eq} (Fig. 2) satisfies the BDP only for low momenta. For higher momenta there is a component of fourfold symmetry in the p_x, p_z section. The momentum density difference at R_{eq} shows that in the formation of a bond the expectation value of the momentum is increased. Additionally, local maxima in $\Delta\pi(\mathbf{p})$ (Fig. 4) occur around $\mathbf{p} = (0,\ 0,\ \pm 1.3)$ and $\mathbf{p} = (\pm 1.3,\ 0,0)$, which indicates a buildup of momentum density which is strongly aligned either along or perpendicular to the p_z axis (but intermediate angles tend to be avoided).

At $R = 4$ the density increase observed in the external region observed at R_{eq} has disappeared, and the fourfold component is more pronounced.

1. Isotropic Husimi function

At all values of k studied, $\Delta\bar{\eta}(\mathbf{q},k)$ evaluated at $R = 4$ showed the expected reduction in electron density in the external region and increase in density in the internuclear region. As k was increased, the region of depleted density in this forward-type distribution moved toward the core region. At R_{eq} the situation is markedly different, and we must go to the anisotropic Husimi function to study the phase-space density.

2. Anisotropic Husimi function

Figure 13 includes two phase-space cross sections obtained by setting all but either q_z and k_x or q_z and k_z equal to zero. At all values of transverse $\mathbf{k}$ above about 1.5 studied, only forward density redistribution is seen. For values of k_x less than 1.5 reverse redistribution is observed.

Similarly, for k_z between zero and 1.5 the region is characterized by reverse density redistribution. However for k_z in the range of 1.5 to 2.8 only global increase in electron density occurs, and for k_z between 2.8 and 4.7 there is a recurrence of the reverse redistribution. At higher values of k_z studied only global increase in density is seen.

The above findings lead to a modified form of the BDP. For we do find an increased probability of finding electrons whose momentum is transverse—but only in the internuclear region. On the other hand, there is an increase probability of finding electrons moving logitudinally in the external region. This increased preference in the directionality of the momentum was observed in $\Delta\pi(\mathbf{p})$ as discussed above.

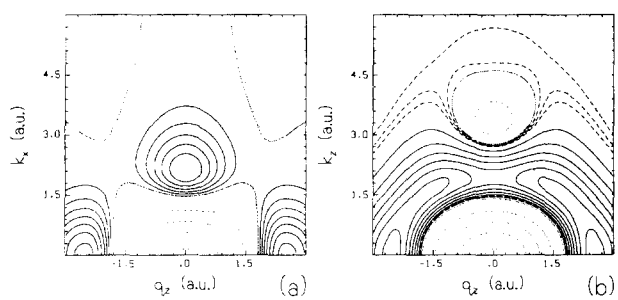

FIG. 13. Husimi function sections for N_2 at R_{eq}: (a) q_z,k_x section with $q_x = q_y = 0$, $k_y = k_z = 0$ and (b) q_z, k_z section with $q_x = q_y = 0$, $k_x = k_y = 0$. Contours: (a) dotted lines: -4×10^{-3} to 0 in steps of 10^{-3}; solid lines: 1×10^{-4} to 7×10^{-4} in steps of 10^{-4}; widely space dotted lines: -3×10^{-6} to -1×10^{-6}, (b) dotted lines and solid lines: same as in (a); dashed lines 1×10^{-5} to 3×10^{-5} in steps of 10^{-5}.

Further corroboration of this result is given by the data shown in Fig. 14. Figure 14(a) is a section of the Husimi phase space defined by setting $\mathbf{q} = (0, 0, 0)$ and $k_y = 0$. At this point, which is centered between the two nuclei, one sees an increased density of electrons whose momentum is transverse. Figure 14(b) is similar to Fig. 14(a), except we have set $q_z = 1.5$, which is a point in the external region. This section of the phase space reveals an increased density of electrons moving longitudinally. Since $\pi(\mathbf{p})$ is related to contributions from these and other similar sections we see how it is that the BDP may be weakened, and how it is that a p_x, p_z section of $\pi(\mathbf{p})$ has nearly fourfold symmetry.

VII. SUMMARY

We have studied the one-electron position, momentum, and phase-space densities of H_2, LiH, and N_2. In many, but not all, instances we observed the expected "forward redistribution" of density—i.e., a shift of density in coordinate space into the internuclear region as a bond is formed, and the BDP—a preferential orientation of momentum transverse to the bond. In some cases these effects do not occur or are obscured. It was found that the Husimi function provides a physical means of decomposing both $\rho(\mathbf{r})$ and $\pi(\mathbf{p})$ in terms of either momentum or position labels, thereby providing additional information.

Our study of density difference plots revealed that a region of reduced electron density in $\Delta\rho(\mathbf{r})$ may, when analyzed by means of $\Delta\eta$, correspond to a region of reduced density over one range of momenta and increased density in another range of momenta. The same may be said of regions of increased electron density in $\Delta\rho(\mathbf{r})$, and of increases and decreases in momentum density found in $\Delta\pi(\mathbf{p})$. In this regard, the Husimi function provides more information about electron density rearrangements which occur in the formation of a bond.

The absence of an apparent BDP for LiH is not surprising, given the polar nature of the bond. In N_2, however, the situation is more complicated. If we examine the momentum distribution for electrons in the internuclear region, we find a BDP. It is attenuated in the total momentum density by contributions from other spatial regions where the distribution may be isotropic or other directions preferred. In the external region, longitudinal orientation is preferred and the total momentum density for N_2 thus has a significant component of near fourfold symmetry. In polyatomic molecules the momentum density is likely to have few clear features, because of superimposed contributions from different regions. The Husimi function provides a way of separating these contributions and recovering a more understandable description.

Although our investigations have been purely theoretical, it is important to recall that the Husimi function is in principle observable. The decompositions we have discussed thus have a physical basis and are not properties of a particular theoretical model, as are decompositions based on separation of orbital contributions.

In the case of atomic Husimi functions,[10] it was found that most of the important information about atomic electron distributions is contained in the angle-averaged Husimi function. In the present molecular systems we found that, qualitatively, the angle-averaged Husimi function differed only slightly from the full Husimi function for H_2 and LiH. This is an indication that the electron phase space density varies little with changes in the orientation of the momentum vector. For N_2 evaluated at R_{eq} this was not the case. We found the phase-space density to be strongly dependent on the orientation of $\mathbf{k}$ in some regions of phase space, and hence the isotropic Husimi function does not provide an adequate description of this system. It appears likely that for at least some polyatomic systems the full, six-dimensional Husimi function will be necessary. We are investigating various ways of looking at this function, including the use of a "natural density pair" expansion,[11,32] in which the Husimi function is expanded as a sum of products of coordinate and momentum densities which can be examined individually.

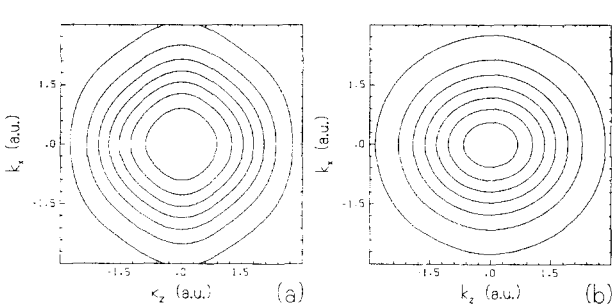

FIG. 14. Husimi function k_x, k_z sections (wtih $k_y = 0$) for N_2 at R_{eq}: (a) $\mathbf{q} = (0,0,0)$ and (b) $\mathbf{q} = (0,0,1.5)$. Contours: (a) 1×10^{-3} to 7×10^{-3} in steps of 10^{-3}, (b) same as (a).

ACKNOWLEDGMENTS

The work reported in this paper was supported by the National Science Foundation through Grant No. CHE-8519723. Calculations were performed on the VAX 8650 computer in the Department of Chemistry of the University of Wisconsin-Madison. Programs used in plotting sections of the full Husimi function were originally written by Mark E. Casida.

[1] It is sometimes suggested that a wave function can be obtained from x-ray data [see, e.g., L. Massa, M. Goldberg, C. Frishberg, R. F. Boehm, and S. J. LaPlaca, Phys. Rev. Lett. **55**, 662 (1985)] but this depends on use of a model wave function that is sufficiently restricted that the parameters determining it are uniquely defined by the resultant density. [J. E. Harriman, Phys. Rev. A **34**, 29 (1986); M. Levy and J. A. Goldstein, Phys. Rev. B **35**, 7887 (1987)].

[2] See, e.g., *Electron Densities and the Chemical Bond*, edited by P. Coppens and M. B. Hall (Plenum Press, New York, 1982).

[3] See, e.g., M. J. Cooper, Rep. Phys. **48**, 415 (1985).

[4] See, e.g., C. E. Brion, Int. J. Quantum Chem. **29**, 1397 (1986), and references cited therein.

[5] The term "correlation" is usually used in quantum chemistry to refer to the difference between an exact, nonrelativistic result and the corresponding Hartree–Fock approximation. In the more general statistical sense, a joint distribution includes correlation if it is not factorable into a product of independent distributions.

[6] E. Wigner, Phys. Rev. **40**, 749 (1932).

[7] A marginal of a joint distribution is obtained by integrating over one (set of) variable(s). It gives the distribution for the remaining variable(s).

[8] L. Cohen, in *NATO Advanced Study Institute on Frontiers of Nonequilibrium Statistical Physics*, edited by G. T. Moore and M. O. Scully (Plenum, New York, 1986).

[9]For clarity we reserve the symbols r and p to represent phase-space variables, and the symbols q and k to denote the locations of the centers of the Gaussian wave packets in phase space. Note that r and q have the same dimensions, but p and k are related by the equation $p = \hbar k$. Since we use atomic units throughout this paper this distinction is inconsequential.
[10]M. E. Casida, J. E. Harriman, and J. L. Anchell Int. J. Quantum Chem. Symp. **21**, 435 (1987).
[11]J. E. Harriman, J. Chem. Phys. **88**, 6399 (1988).
[12]This definition of the Husimi function differs from the definition given in previous papers (Refs. 10 and 11) by the normalization factor of $1/(2\pi)^3$. This distinction is emphasized by the use of the symbol η rather than C used in our earlier work.
[13]A. Royer, Phys. Rev. Lett. **55**, 2745 (1985).
[14]See also J. P. Dahl, Physica A **114**, 439 (1982); Phys. Scr. **25**, 499 (1982) and references cited therein.
[15]P. A. M. Dirac, *Quantum Mechanics*, 4th ed. (Oxford University, Oxford, 1958), pp. 36, 37.
[16]Relationships among the density matrix, Wigner function, and Husimi function, and the recovery of the Wigner function from the Husimi function are discussed in Ref. 10 and 11.
[17]While e, $2e$ experiments are usually interpreted in terms of orbital contributions, this is based on a Hartree Fock–Koopmans' theorem-like analysis.
[18]6-311G and 6-311G** bases are described by R. Krishna, J. S. Binkley, R. Seeger, and J. A. Pople, J. Chem. Phys. **72**, 650 (1980).
[19]GAUSSIAN 82 is an *ab initio* program developed by J. S. Binkley, M. J. Frisch, D. J. Defreas, K. Raghavachri, R. A. Whiteside, M. B. Schlegel, E. M. Floder, and A. J. Pople, Carnegie-Mellon University, Pittsburgh, PA.
[20]The original version of the program GAMESS was created by M. Dupuis, P. Spangler, and J. J. Wenddowski, NRCC Software Catalog, Vol. 1, Program GG01 (1980). It was later modified by M. Schmidt and M. Gordon.
[21]A. J. Thakkar, A. M. Simas, and V. H. Smith, Jr., J. Chem. Phys. **81**, 2953 (1984).
[22]See, e.g., K. Ruedenberg, Rev. Mod. Phys. **34**, 326 (1962).
[23]See, e.g., I. N. Levine, *Quantum Chemistry, III* (Allyn and Bacon, Boston, 1983), p. 398.
[24]C. A. Coulson, Proc. Cambridge Philos. Soc. **37**, 55 (1940).
[25]For further discussion and additional references, see A. C. Tanner, Chem. Phys. **123**, 241 (1988).
[26]Although this example involves a simple expression for a bonding molecular orbital, qualitative details of this result can be reproduced using more complicated wave functions. The calculation is trival, for example, for a "full CI" treatment with a single 1s Gaussian on each atom in H_2.
[27]P. Kaijser and P. Lindner, Philos. Mag. **31**, 871 (1975).
[28]S. R. Langhoff and R. A. Tawil, J. Chem. Phys. **63**, 2745 (1975).
[29]I. R. Epstein and A. C. Tanner, in *Compton Scattering*, edited by B. Williams (McGraw-Hill, New York, 1977).
[30]Note that the angle-averaged Husimi function evaluated at $k = 0$ is identical to the anisotropic Husimi function evaluated at $\mathbf{k} = (0, 0, 0)$.
[31]M. J. Feinberg and K. Ruedenberg, J. Chem. Phys. **34**, 1495 (1971).
[32]J. E. Harriman (to be published).